

## **THERMAL BEHAVIOUR OF TITANIA BASED MATERIALS**

### **Mathematical modeling of emanation thermal analysis results**

*V. Balek<sup>1</sup>, V. Zelenák<sup>1\*</sup>, T. Mitsuhashi<sup>2</sup>, I. N. Beckman<sup>1\*\*</sup>, H. Haneda<sup>2</sup> and P. Bezdička<sup>3</sup>*

<sup>1</sup>Nuclear Research Institute, CZ-250 68 Ře , Czech Republic

<sup>2</sup>National Institute for Materials Science (NIMS), 1-1 Namiki, Tsukuba 305-0044, Ibaraki, Japan

<sup>3</sup>Institute of Inorganic Chemistry, Academy of Sciences of the Czech Republic, 250 68 Ře , Czech Republic

#### **Abstract**

Emanation thermal analysis (ETA) was used in the characterization of microstructure changes during heating of precursors for the titania based materials: hydrous titania,  $\text{TiO}_2 \cdot n\text{H}_2\text{O}$  ( $n=0.58$ ) and hydrous titania containing 10% ruthenia,  $(\text{TiO}_2)_{0.9}(\text{RuO}_2)_{0.1} \cdot n\text{H}_2\text{O}$  ( $n=1.5$ ). The precursors were heated at the constant rate  $6 \text{ K min}^{-1}$  in argon flow in the range 20–1000°C. ETA results were compared with the theoretical curves simulating the temperature dependences of radon release rate,  $E(T)$ . Two mathematical models were used in the simulation. The models considered either subsequent or simultaneous solid state processes (i.e. dehydration, crystallization or phase transition, resp.) during thermal treatment of titania based materials. A good agreement was found between experimental and the simulated ETA curves. The results of ETA were confirmed by XRD patterns of intermediate products of thermal treatment of the precursors.

**Keywords:** emanation thermal analysis, hydrous titania, mathematical modeling, XRD

#### **Introduction**

A wider application of titania as photosensitive material is limited by the fact that the wavelength lower than 420 nm is needed for its effective practical photocatalytic use [1]. One of the ways how to reach this requirement is the addition of transition metals and metal oxides as ‘dopants’ to titanium dioxide, so that the range of the photochemical response of the material will expand making use of light in the visible region [2–4].

The photoactive materials usable in a broader wavelength region have been prepared by a number of authors e.g. [5]. In our previous paper we have reported the

\* On leave from the Department of Inorganic Chemistry, Faculty of Science, P. J. Šafárik University, 041 54 Košice, Slovak Republic

\*\* On leave from the Department of Chemistry, Moscow State University, 199 234 Moscow, Russia

method of the preparation of titania based photoactive materials, containing 10% ruthenia [6]. The dehydration of hydrous oxides used as precursors for the preparation of the photoactive materials was characterized by means of thermogravimetry. The emanation thermal analysis was used [6] for the first time in order to monitor microstructure changes taking place under *in situ* conditions used for the preparation of titania based photocatalysts.

The aim of this study is to compare the experimental results of emanation thermal analysis (ETA) with the results of the mathematical modeling. The recently developed model was used for the evaluation of the experimental results of ETA. The results of XRD were used to demonstrate a good reliability of the results obtained by modeling.

## Experimental

### *Preparation of hydrous oxides*

Reagent grade  $\text{RuCl}_3 \cdot n\text{H}_2\text{O}$  (Furuya Metal) and  $\text{TiCl}_4$  (Kanto Chemicals) were used as starting materials for the preparation of hydrous oxides of the formulae  $\text{TiO}_2 \cdot 0.58\text{H}_2\text{O}$  and  $(\text{TiO}_2)_{0.9}(\text{RuO}_2)_{0.1} \cdot 1.5\text{H}_2\text{O}$ , resp. Titanium chloride solution was prepared by dissolving  $\text{TiCl}_4$  in a 0.1 M hydrochloric acid. For the preparation of hydrous titania-ruthenia samples the solutions of the dissolved Ti and Ru chlorides in the Ti:Ru ratio 9:1 were used. The solutions were added by drops to the 2 M ammonia. The precipitates of the hydrous oxides obtained in this way were washed, filtered and dried at 120°C.

### *Methods used*

The apparatus used for the ETA-DTA measurements was constructed on the basis of the Netzsch DTA 409 Equipment. The sample amount of 0.1 g was placed into a corundum crucible situated in a furnace heated at the rate of 6 K  $\text{min}^{-1}$ , being overflowed during the measurement by the constant flow of argon, which carried the radon released from the sample into the measuring chamber of radon radioactivity.

XRD patterns were recorded with a PHILIPS diffractometer using  $\text{CuK}_\alpha$ , Ni-filtered radiation.

### *Principles of the mathematical modeling*

The mathematical model used in this study is based on the principles described by Beckman and Balek in [7].

Following dependences were considered in the construction of the thermal dependences of radon release rate in this study:

$$E(T) = E_R + \sum_i E_i(T) \quad (1)$$

$$E_i(T) = A_i D_i(T) S_i(T), \text{ where } i = 1, 2 \quad (2)$$

$E_R$  is the value of radon release rate due to the recoil, corresponding to the experimental value of  $E$  measured at room temperature,  $A$  is the pre-exponential factor, function  $D_i(T)$  reflects the temperature dependence of radon diffusion considering validity of the Arrhenius law

$$D_i(T) = D_{i0} \exp(-Q_i/RT) \quad (3)$$

In this function,  $Q_i$  is the activation energy of radon diffusion in the respective solids;  $D_{i0}$  is the pre-exponential factor characterizing the lattice properties of the solids.

$S_i(T)$  is an integral Gauss function expressing the temperature dependence of changes of the surface area and open porosity serving for the radon migration

$$S_i(T) = 1 - 0.5[1 + \operatorname{erf}(z)] \quad (4)$$

where

$$\operatorname{erf}(z) = \frac{2}{\sqrt{\pi}} \int_0^z \exp(-z^2) dz \quad (5)$$

where  $\operatorname{erf}(z)$  is the integral Gauss function of  $z$ ,  $z = \frac{T - T_m}{\sigma 2^{1/2}}$ ,  $\sigma = \frac{\Delta T}{3}$ ,  $T_m$  is the temperature corresponding to the maximal rate of the  $S_i(T)$  change,  $\Delta T$  is the width of the temperature range in which  $S_i(T)$  takes place.

## Results and discussion

### *TiO<sub>2</sub>·0.58H<sub>2</sub>O*

According to TG, DTA and TEM results [6], the mass loss observed in the range from 40 to 420°C during heating of the hydrous titania in argon is due to the sample dehydration. From the value of the total mass loss 11.5%, it was determined that the amount of water present in the sample corresponded to  $n=0.58$ .

The information about the microstructure changes of the sample taking place on heating of hydrous titania under *in situ* conditions was obtained from ETA results (Fig. 1, curve 1).

In Fig. 1 there are represented the experimental ETA results of hydrous titania (nominal composition  $\text{TiO}_2 \cdot 0.58\text{H}_2\text{O}$ ) in comparison with the model ETA curves designed under two different assumptions, namely (a) that the dehydration and the phase transition took place as subsequent processes and (b) that the dehydration and the phase transition took place as simultaneous processes in parallel.

From the experimental ETA curve it follows that during heating from 20 to 330°C the enhanced radon release rate was observed as a consequence of the microstructure changes accompanying the dehydration of the sample.

The following decrease of radon release rate,  $E$ , in the range 330–800°C was attributed to the growth of primary anatase grains and consequent decreasing of the sample surface area. This finding is in accordance with TEM and surface area measurements [6].

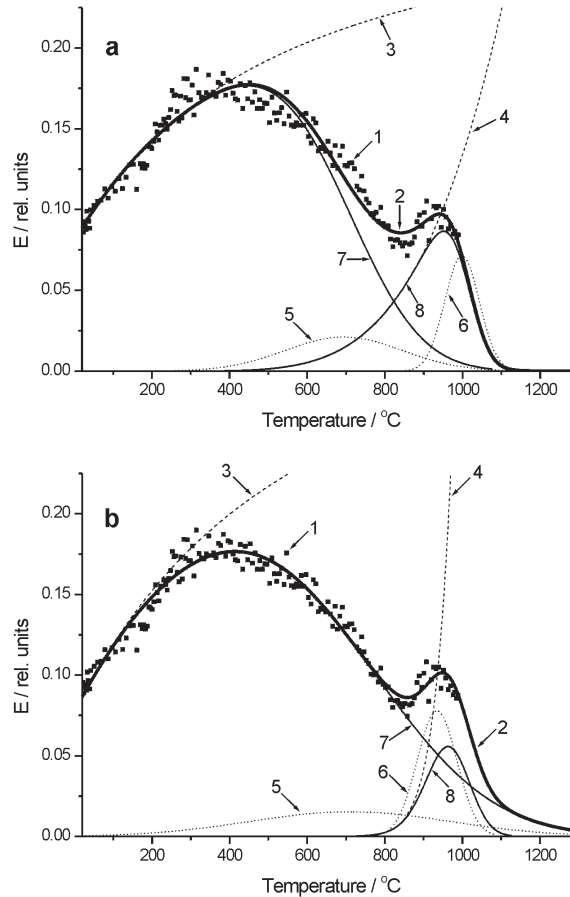


**Fig. 1** Thermal behavior of  $\text{TiO}_2 \cdot 0.58\text{H}_2\text{O}$  characterized by emanation thermal analysis during heating in argon. The comparison of the experimental results with the simulated ETA curves using (a) approach of subsequent, (b) simultaneous processes; 1 – experimental results; 2 – the overall model curve of the temperature dependence of  $E(T)$ ; 3, 4 – diffusion component  $D_1(T)$  and  $D_2(T)$  used in the modeling; 5, 6 – derivatives of respective S-like shape functions  $S_i(T)$  which characterize the changes of the structure irregularities, serving as paths for the radon migration; 7, 8 – the model curves  $E_1(T)$  and  $E_2(T)$  describing the process of dehydration and the phase transition anatase–rutile, resp.

The increase of the radon release rate,  $E$ , in the range 800–950°C corresponded to the onset of anatase-rutile phase transition indicating the increased structural disorder in this temperature range. The decrease of  $E$  above 950°C reflected the formation of a well-crystallized rutile.

The mathematical model used for the more detailed description and evaluation of the ETA curves is based on two different approaches. In the first one it was considered that the dehydration and anatase-rutile phase transition took place subsequently

as independent processes. In the second approach it was considered that dehydration and phase transition take place simultaneously. The parameters used in the mathematical models under both considerations are summarized in Table 1. Figure 1 demonstrates the comparison of the experimental and the model ETA curves.

**Table 1** Values of activation energy  $Q$  of radon migration in the near surface layers of titania precursor determined from the mathematical models using two different approaches

Approach 1: subsequent processes			
	$Q/\text{kJ mol}^{-1}$	$T_m/^\circ\text{C}$	$\Delta T/^\circ\text{C}$
$E_1$	6.1	445	706
$E_2$	148.8	952	202
Approach 2: simultaneous processes			
	$Q/\text{kJ mol}^{-1}$	$T_m/^\circ\text{C}$	$\Delta T/^\circ\text{C}$
$E_1$	7.2	413	785
$E_2$	588.2 (not reliable)	964	134

As it follows from Fig. 1 a good fit of the experimental ETA curve was obtained for both approaches. The overall model ETA curve, representing the temperature dependence of  $E(T)$ , (Fig. 1, curve 2) is the sum of the model curve  $E_1(T)$  (Fig. 1, curve 7) and the model curve  $E_2(T)$  (Fig. 1, curve 8). As it follows from Eq. (2), the  $E_i(T)$  dependences ( $i=1, 2$ ) were obtained as the product of diffusion components  $D_i(T)$  (Eq. (3)) and  $S_i(T)$  (Eq. (4)). The  $D_i(T)$  model curves are demonstrated in Fig. 1 as curves 3 and 4, resp. The S-like shape functions  $S_i(T)$  characterized the changes of surface area and open porosity serving for the radon migration during the respective solid-state processes. Curves 5 and 6 in Fig. 1 are the derivatives of these S-like shape functions giving an idea about the rate of the changes of the structure irregularities in the titania sample, serving as paths for the radon migration.

From the parameters presented in Table 1 it follows that both models reflect the process of dehydration  $E_1(T)$  similarly. Temperatures  $T_m=455$  and  $413^\circ\text{C}$ , resp. corresponding to the maximal radon release rate, agree with the TG results [6]. From TG curves presented in [6] it followed that the major part of the water was released up to  $420^\circ\text{C}$ . The values of activation energy  $Q$  ( $6.1$  and  $7.2 \text{ kJ mol}^{-1}$ ) of radon migration in the near surface layers calculated from the proposed mathematical models are similar.

As to the radon migration in the near surface layers in the temperature range  $800\text{--}950^\circ\text{C}$ , where anatase-rutile phase transition takes place, we assumed that the approach of two simultaneous processes is more reliable for the determination of activation energy values  $Q=148.8 \text{ kJ mol}^{-1}$ .

XRD patterns (Fig. 2) demonstrated that the initial hydrous titania sample, used for the thermal treatment was poorly crystalline anatase. No differences were observed between initial sample and the sample heated to  $300$  and  $500^\circ\text{C}$ . It followed from Fig. 2 that after heating to  $800^\circ\text{C}$  the phase transition from anatase to rutile took place although the

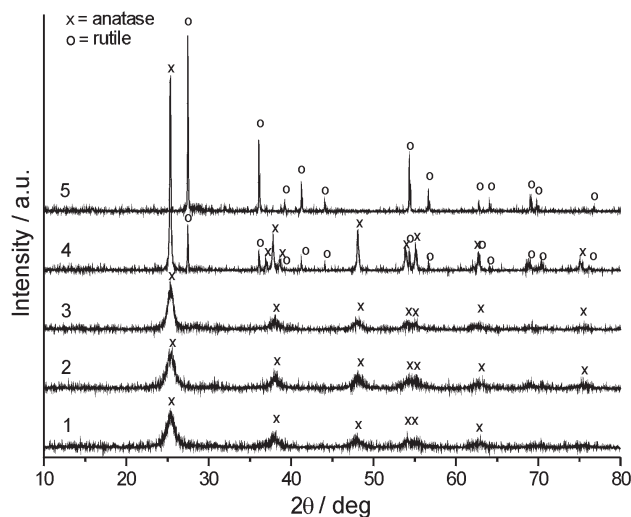
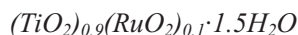


**Fig. 2** XRD patterns of  $\text{TiO}_2 \cdot 0.58\text{H}_2\text{O}$  heated in argon 1 – initial sample, 2 – sample heated to  $300^\circ\text{C}$ , 3 – to  $500^\circ\text{C}$ , 4 – to  $800^\circ\text{C}$  and 5 – to  $1100^\circ\text{C}$

diffraction lines of both, rutile and anatase were present in the XRD patterns of the sample. This is in agreement with the model ETA curve 8 in Fig. 1. Finally, from Fig. 2 it follows that after heating to  $1100^\circ\text{C}$  only a well-crystalline rutile was found in the XRD pattern, which is in agreement with model ETA curve 8 in Fig. 1.



It was reported in our previous paper [6] that the mass loss of the sample due to dehydration observed on heating from  $50$ – $1000^\circ\text{C}$  corresponds to the amount  $1.5$  mol  $\text{H}_2\text{O}$  present in the hydrous oxide.

The different stages of the sample dehydration were characterized by ETA as follows (Fig. 3, curve 1): the enhanced release of radon indicating the liberation of surface and open pores from adsorbed water molecules in the temperature interval  $50$ – $240^\circ\text{C}$ , corresponds to the release of water from surface and intergranular space. On further heating in the range  $240$ – $450^\circ\text{C}$  the decrease of the radon release rate indicated the annealing of surface and porosity in the near surface layers from where the water molecules were released during the heating up to  $240^\circ\text{C}$ . The decrease of  $E$  characterizes the decrease of the number of diffusion channels e.g. open porosity serving for the radon migration area available for the radon diffusion. ETA reflected this process as a decrease of the radon release rate  $E$  in spite of the fact that the water release from the bulk of the sample was indicated by TG. The decrease of  $E$  continued up to  $580^\circ\text{C}$ , characterizing the intensity of the annealing of diffusion channels for radon.

The slight increase of  $E$  observed above  $580^\circ\text{C}$  reflected microstructure changes of the titania-ruthenia sample  $(\text{TiO}_2)_{0.9}(\text{RuO}_2)_{0.1} \cdot 1.5\text{H}_2\text{O}$  due to the formation of metastable dehydrated product and indicated the onset of the crystallization. We suppose

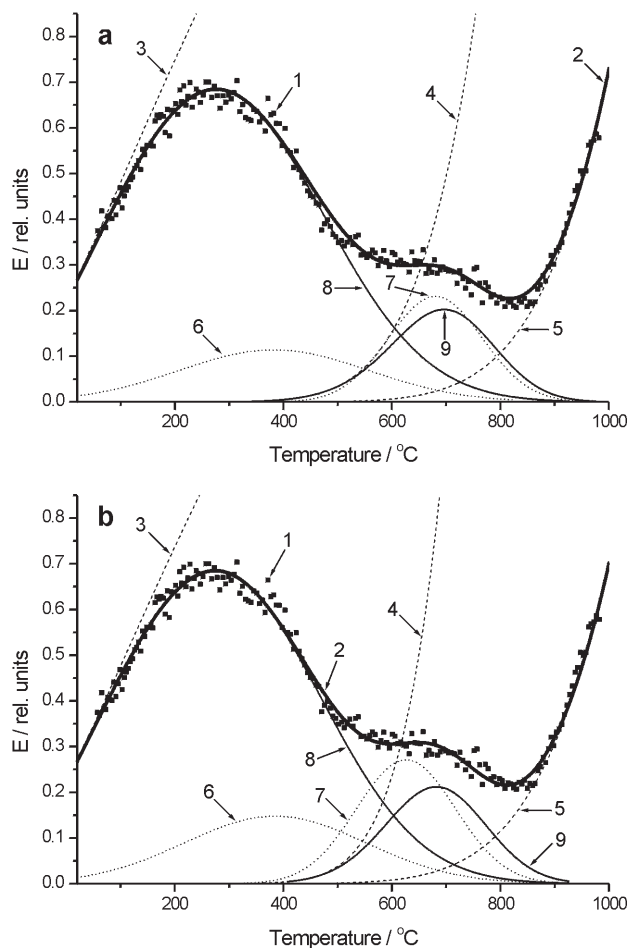


**Fig. 3** Thermal behavior of  $(\text{TiO}_2)_{0.9}(\text{RuO}_2)_{0.1} \cdot 1.5\text{H}_2\text{O}$  characterized by emanation thermal analysis during heating in argon. The comparison of the experimental results with the simulated ETA curves using (a) approach of subsequent, (b) simultaneous processes; 1 – experimental results; 2 – the overall model curve of the temperature dependence of  $E(T)$ ; 3, 4, 5 – diffusion component  $D_1(T)$ ,  $D_2(T)$  and  $D_3(T)$  used in the modeling; 6, 7 – derivatives of respective S-like shape functions  $S_i(T)$  which characterize the changes of the structure irregularities, serving as paths for the radon migration; 8, 9 – the model curves  $E_1(T)$  and  $E_2(T)$  describing the process of dehydration and the phase transition anatase–rutile, resp.

that the radon atoms trapped in the amorphous samples are released during the crystallization and annealing of structure irregularities being indicated as increase of  $E$ . Further decrease of  $E$  indicated the formation of a more ordered structure containing lower concentration of structure defects serving as radon diffusion paths. The in-

crease of  $E$ , observed above 830°C, indicated the temperature of the onset of the diffusion release of radon from the sample.

In the evaluation of the ETA results similar mathematical models were used as described in previous paragraphs (Eqs (2)–(5)). However, in contrast to hydrous titania, three processes were considered in the thermal treatment of  $(\text{TiO}_2)_{0.9}(\text{RuO}_2)_{0.1} \cdot 1.5\text{H}_2\text{O}$ . The first process  $E_1(T)$  is due to sample dehydration, the second process  $E_2(T)$  is due to sample crystallization and the third process  $D_3(T)$  is due to bulk diffusion of radon above the Tammann temperature. The parameters determined from the designed models are summarized in Table 2. Figure 3 demonstrates the comparison of the experimental and model ETA curves for  $(\text{TiO}_2)_{0.9}(\text{RuO}_2)_{0.1} \cdot 1.5\text{H}_2\text{O}$ .

**Table 2** Values of activation energy  $Q$  of radon migration in the near surface layers of titania-ruthenia precursor determined from the mathematical models using two different approaches

Approach 1: subsequent processes			
	$Q/\text{kJ mol}^{-1}$	$T_m/^\circ\text{C}$	$\Delta T/^\circ\text{C}$
$E_1$	12.9	275	454
$E_2$	166.2	696	225
$D_3$	217.1	–	–
Approach 2: simultaneous processes			
	$Q/\text{kJ mol}^{-1}$	$T_m/^\circ\text{C}$	$\Delta T/^\circ\text{C}$
$E_1$	12.82	274	447
$E_2$	203.9	682	218
$D_3$	205.5	–	–

It is of interest to see that the application of both approaches resulted in the similar values of activation energy  $Q$  of radon migration in the near surface layers, as well as in the temperatures of the maximal radon release rate and the half width of the simulated ETA effects. Nevertheless, the model approach, which considers the subsequent processes of dehydration and crystallization, can be considered as more reliable. The activation energies  $Q$  calculated by this model are:  $Q_1=12.9 \text{ kJ mol}^{-1}$ ,  $Q_2=166.2 \text{ kJ mol}^{-1}$ ,  $Q_3=217.1 \text{ kJ mol}^{-1}$ . We should mention that the values of activation energy  $Q$ , characterizing the permeability of the diffusion paths for radon are different due to the solid state processes in the respective temperature ranges. In view of the character of the solid state processes the determined values of  $Q_1$ ,  $Q_2$ ,  $Q_3$  can be seen more realistic than the corresponding values calculated when the model approach of the simultaneous processes was used (Table 2).

A good correlation was obtained when comparing the simulated temperature dependences of  $E(T)$  with the experimental ETA results for the sample  $(\text{TiO}_2)_{0.9}(\text{RuO}_2)_{0.1} \cdot 1.5\text{H}_2\text{O}$ . XRD patterns were measured in order to check the real structure and microstructure development on heating.

XRD patterns (Fig. 4) of the initial hydrous titania-ruthenia oxide and the sample heated to 400°C revealed a poorly crystalline character of both samples. Anatase,



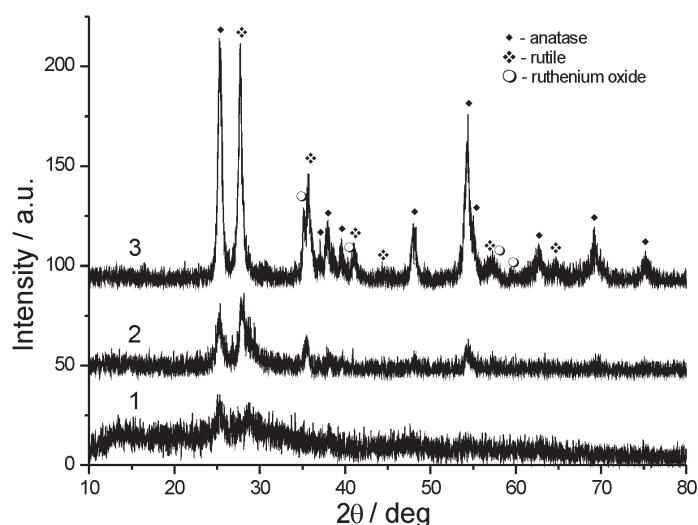


**Fig. 4** XRD patterns of  $(\text{TiO}_2)_{0.9}(\text{RuO}_2)_{0.1} \cdot 1.5\text{H}_2\text{O}$  heated in argon 1 – initial sample, 2 – sample heated to 400°C and 3 – to 600°C

rutile and ruthenium oxide were identified by XRD patterns in the sample heated to 600°C. XRD results confirmed the temperature dependence of  $E(T)$  from where the crystallization onset at 400°C was evaluated by the mathematical model (Fig. 3, curve 9).

## Conclusions

The reliability of the designed mathematical model was confirmed by the good agreement with the experimental data of ETA for both hydrous titania based samples, which characterized the microstructure development during their dehydration crystallization and phase transition from anatase to rutile. The parameters used in the simulated temperature dependences of the radon release rate for the description of the above processes enabled us to compare intensity of the development of the surface area and structure irregularities serving for the radon migration. The approach used in this study can be used for the evaluation of ETA data in the case of thermal decomposition of solids accompanied by the formation of the active surface. ETA can be advantageously used to test the thermal stability of the intermediate products in the preparation of materials where the active surface is the requested property (photocatalysts, catalysts etc.).

\* \* \*

This work was supported by the Grant Agency of the Czech Republic (Project 104/00/1046), by the Ministry of Education of the Czech Republic (project ME180) and by the Science and Technology Agency of Japan (in the frame of the Cross-Over Project in support of Nuclear technology). The authors (V. Z. and I. N. B.) thank the NATO Science Fellowships Program for the financial support.

## References

- 1 A. Fujishima and K. Honda, *Nature*, 37 (1972) 238.
- 2 D. Bockelmann, R. Goslich and D. Bahnemann, In: *Solar Thermal Energy Utilization*, M. Becker, K.-H. Funken and G. Schneider, Eds, Springer Verlag GmbH, Heidelberg, 1992, Vol. 6, p. 397.
- 3 L. Palmisano, V. Augugliaro, A. Sclafani and M. Schiavello, *J. Phys. Chem.*, 92 (1988) 6710.
- 4 E. Borgarello, J. Kiwi, M. Grätzel, E. Pelizzetti and M. Visca, *J. Am. Chem. Soc.*, 104 (1982) 2996.
- 5 J. Málek, A. Watanabe and T. Mitsuhashi, *Thermochim. Acta*, 282/283 (1996) 131.
- 6 V. Balek, E. Klosová, J. Málek, J. Šubrt, J. Boháček, P. Bezdička, A. Watanabe and T. Mitsuhashi, *Thermochim. Acta*, 340/341 (1999) 301.
- 7 I. N. Beckman and V. Balek, *J. Therm. Anal. Cal.*, 67 (2002) 49.